Received 12 June 2017; revised 21 July 2017 and 16 August 2017; accepted 9 September 2017. Date of publication 20 September 2017; date of current version 24 October 2017. The review of this paper was arranged by Editor A. G. U. Perera.

Digital Object Identifier 10.1109/JEDS.2017.2751554

Fabrication and Characterization of Ultra-wide Bandgap AlN-Based Schottky Diodes on Sapphire by MOCVD

HOUQIANG FU, XUANQI HUANG, HONG CHEN, ZHIJIAN LU, AND YUJI ZHAO (Member, IEEE)

1 School of Electrical, Computer, and Energy Engineering, Arizona State University, Tempe, AZ 85287, USA

CORRESPONDING AUTHOR: Y. ZHAO (e-mail: yuji.zhao@asu.edu).

This work was supported in part by the Defense Threat Reduction Agency Young Investigator Award under Grant HDTRA11710041, in part by the Kyma Technologies, and in part by the LeRoy Eyring Center for Solid State Science at Arizona State University.

ABSTRACT AlN Schottky diodes with various device geometries were fabricated on sapphire substrate and their temperature-dependent current–voltage characteristics were analyzed. At forward bias, high ideality factors were obtained, indicating a large deviation from the ideal thermionic emission model. At reverse bias, the breakdown voltage showed a negative temperature dependence, and the leakage current was well described using a 2-D variable-range hopping conduction model. Furthermore, the breakdown voltages and leakage currents of the devices showed a strong dependence on the surface distance between the ohmic and Schottky contacts, but a relatively small dependence on the area of the Schottky contacts. These results suggest surface states between ohmic and Schottky contacts play a more important role than the metal/AlN interface in determining the reverse breakdown and leakage current of AlN Schottky diodes. A quantitative study of AlN Schottky diodes at high temperature reveals a geometry-dependent surface breakdown electric field and surface leakage current. Surface passivation and treatments may enhance the device performances and impact the reverse breakdown and current leakage mechanisms. These results will serve as the guidance for the design and fabrication of future AlN electronic devices.

INDEX TERMS Aluminum nitride, Schottky diodes, surface states, ideality factor, breakdown, current leakage, hopping conduction.

I. INTRODUCTION

Wurtzite (In, Ga, Al)N wide bandgap III-nitride semiconductors have been widely exploited in optoelectronic devices such as laser diodes (LDs) [1], light-emitting diodes (LEDs) [2]–[7], photovoltaics (PVs) [8], [9], nonlinear optics [10], and photodetectors (PDs) [11], [12], as well as in electronic devices such as high electron mobility transistors (HEMTs) [13], high power PN diodes [14], [15] and Schottky diodes [16]. Among all the III-nitride materials, AlN has the largest bandgap, largest critical electric field, highest thermal conductivity, and most stable high temperature performance [17], [18]. These superior material properties make AlN an attractive candidate for high performance electronic devices, especially for high power and high temperature operations such as motor drive, rail tractions, PV inverter, high temperature sensors, space exploration, and so on. However, due to the lack of high quality AlN substrates [19] and challenges in AlN epitaxial growth [20], only limited work has been reported on AlN electronic devices [17]–[19]. Irokawa *et al.* [17] first demonstrated lateral Pt/AlN Schottky diodes directly formed on single crystal AlN substrate. The n-type conductivity was induced by the unintentionally doped oxygen or nitrogen vacancy in AlN, which is very difficult to control and not suitable for real device fabrication. The devices showed off-state current of 2.0×10^{-6} A/cm^2 and breakdown voltage (V_{BD}) of 20–30 V. Furthermore, Kinoshita *et al.* [18] reported 150 μm-thick Si-doped AlN layers on AlN substrate by hydride vapor phase epitaxy (HVPE). Their Ni/AlN vertical Schottky diode had off-state current below 3×10^{-7} A/cm^2 and V_{BD} of 500–800V. In addition, high quality AlN epilayers on low-cost large-size sapphire substrate were also demonstrated using metal organic chemical vapor deposition (MOCVD) [19], [21], which are promising for

commercialization of AlN based electronics. Despite these progress, AlN Schottky diodes have been rarely reported on sapphire substrate [19]. Moreover, a systematical study is still missing on the reverse breakdown and current leakage mechanisms of AlN Schottky diodes, and their high temperature performance is still unclear.

In this work, we report the fabrication and temperature-dependent performances of lateral Pd/n-AlN Schottky diodes on sapphire substrate. At forward bias, large ideality factors were obtained for the AlN Schottky diodes. A negative temperature dependence was observed for the reverse breakdown voltage of the devices, and the leakage current was well described by a 2D-VRH conduction model. Based on these results, it is found that surface states play an important role in the electrical properties of AlN Schottky diodes. Furthermore, surface breakdown electric field and surface leakage current were also obtained for the AlN Schottky diodes, which will serve as comparison references for future design and fabrication of AlN electronic devices.

II. GROWTH, MATERIAL CHARACTERIZATION, AND DEVICE FABRICATION

1-μm-thick Si-doped AlN layer with a nominal Si concentration of 3×10^{18} cm^{-3} was grown by conventional MOCVD on (0001) sapphire substrate. Trimethylaluminum (TMAl) and ammonia (NH_3) were used as precursors for Al and N, respectively. SiH_4 was supplied as n-type dopant Si source. The AlN epilayer was grown at high temperature (~1200°C) after growing AlN buffer layer at a low temperature (LT). More information about the growth can be referenced to Wang *et al.* [22]. The carrier concentration of the AlN epilayer is $\sim 10^{15}$ cm^{-3}. The crystal quality was characterized by high resolution X-ray diffraction (HRXRD) technique using PANalytical X'Pert Pro materials research X-ray diffractometer (MRD) system using Cu Kα radiations. Figure 1(a) shows the (0002) plane rocking curve (RC). The full width at half maximum (FWHM) of (0002) RC of AlN epilayer is 0.16°. The estimated defect density is $>10^9$ cm^{-2} based on methods in [15] and [19]. X-ray photoelectron spectroscopy (XPS) measurements were performed in ultrahigh vacuum system ($<10^{-9}$ Torr) using Al Kα X-ray source. The XPS system is calibrated by C 1s peak (284.6 eV). XPS element analysis confirmed that there is negligible Ga present in the material. This result indicates the sample is indeed AlN instead of AlGaN which is often the case in MOCVD growth of AlN. Figure 1(b) shows the XPS valence band spectrum of the AlN sample. It's assumed that the polarization charge on AlN surface is naturalized by the oppositely charged surface states, resulting in band bending at the surface, i.e., the surface barrier height (SBH) of AlN. Therefore, measuring the SBH of AlN can be used to estimate the density of surface states [23]–[25]. The SBH of the AlN sample at the charge neutrality level (CNL) is given by $(E_g\text{-}E_{VBM}) = 2.60$ eV, where E_g is bandgap of AlN and E_{VBM} is the energy level of valence band minimum (VBM) with respect to the Fermi level at the surface. E_{VBM} was extracted by extrapolating a linear fit of the leading edge of the valance band spectrum to the baseline [26]. The density of surface states is estimated to be 1.1×10^{14} $eV^{-1}cm^{-2}$, which is comparable to previous reports on AlN and larger than that on GaN [20]. The details about the calculation method can be found elsewhere [23].

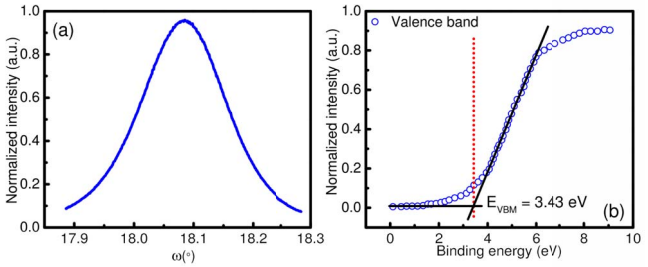

FIGURE 1. (a) Rocking curve of (0002) plane for AlN epilayer. (b) XPS valence band spectrum of the n-AlN sample.

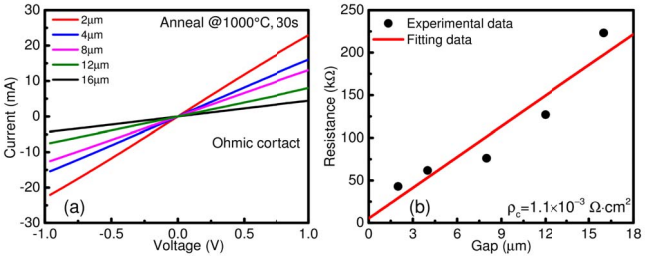

FIGURE 2. (a) TLM I–V characteristics of Ti/Al/Ti/Au contact after annealing. (b) Resistance versus gap of the pads. A linear fitting was performed to extract the contact resistance.

For the ohmic contacts of the devices, Ti/Al/Ti/Au metal stacks were deposited on AlN epilayers using electron beam evaporation and subsequently annealed at 1000°C for 30 seconds in nitrogen ambient using rapid thermal annealing (RTA). The diameter of the circular ohmic contact is 400 μm. Figure 2 shows characterization of the ohmic contacts by transmission line method (TLM). Ti/Al/Ti/Au contacts showed good ohmic behavior after annealing with a contact resistance of 1.1×10^{-3} $\Omega.cm^2$. For Schottky contacts, Pd/Au metal stacks were deposited using electron beam evaporation without thermal annealing process. No passivation or field plate techniques were employed for any AlN Schottky diodes. Figure 3 shows the schematics of the fabricated AlN Schottky diodes with different geometries. The three circular Schottky contacts have a diameters ϕ of 100, 200 and 300 μm, respectively. The side length of the square Schottky contact is 100 μm. The distance between the 200 and 300 μm circular Schottky contacts and the edges of the ohmic contacts is 200 μm. The circular ($\phi = 100\mu m$) and square Schottky contacts are located 50–500 μm away from the edges of the ohmic contacts. The donut-shaped double circle Schottky diodes have ohmic contacts with diameters of 160, 260 and 360 μm. The current–voltage (I–V) characteristics were carried out using a Keithley 4200-SCS parameter analyzer on a thermally controlled probe station.

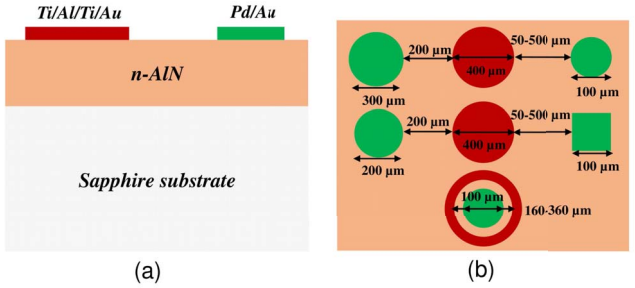

FIGURE 3. Schematic view of (a) the cross-section and (b) top view of Pd/AlN Schottky diodes. The contacts in red are ohmic contact and the contacts in green are Schottky contacts. Schottky contacts are fabricated in three geometries: single circle, square and donut-shaped double circle.

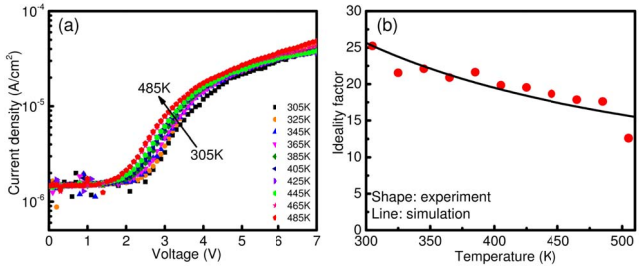

FIGURE 4. (a) Forward I–V characteristics from 305K to 485K and (b) temperature dependence of ideality factor for circular AlN Schottky diodes. The solid circles are experimental results. The dotted line shows the fitting results obtained using Eq. (1).

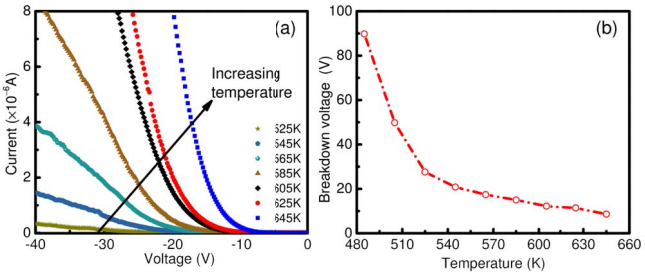

FIGURE 5. (a) Reverse I–V characteristics at high temperatures and (b) breakdown voltage as a function of temperature of circular AlN Schottky diodes.

III. RESULTS AND DISCUSSION

Figure 4(a) presents the I–V curves of AlN Schottky diodes ($\phi = 200\mu m$) at forward bias from 305 K to 485 K. A turn-on voltage of 2.2 V was observed at 305 K, which is very close to the previous reported values [17], [18] and the theoretical Schottky barrier height calculated by Reddy *et al.* [27]. The turn-on voltage decreases from 2.2 V to 1.6 V with increasing temperature, which is possibly due to generated high energy electrons and/or reduced AlN bandgap at high temperatures. The off-state current density is around 1×10^{-6} A/cm^2. The series resistance decreases from 2.0×10^5 Ω to 3.3×10^4 Ω with increasing temperature. Ideally, the I–V characteristics of a Schottky diode are described by thermionic emission model [28]. However, the large ideality factors as shown in Fig. 4(b) suggest that the electron transport mechanism deviates from this model. This is often attributed to the lateral non-uniformities at the Schottky/contact interface [17], [29]. Other contributions from tunneling effects, leakage currents, and defect-related generation and recombination, may also play a role [30]. From a macroscopic perspective, the temperature dependence of the ideality factor, the so-called "T_0 anomaly," is related to the lateral inhomogeneity of the Schottky barrier, which is expressed as [17], [29]:

$$n = 1 + \frac{T_0}{T} \tag{1}$$

where T_0 is a constant related to barrier distribution. A good fitting between the Eq. (1) and the experimental data was obtained.

In Figure 5(a), the temperature-dependent reverse I–V characteristics were measured on AlN Schottky diode ($\phi = 300\mu m$). The breakdown voltage is defined as the threshold voltage at which large reverse current starts to flow in the AlN Schottky diodes. The breakdown mechanism can be determined by the temperature dependence of V_{BD} [31]. If the breakdown is caused by impact ionization, V_{BD}will increase with temperature. This is because the phonon scattering-limited electron mean free path is reduced at higher temperatures, requiring a larger electric field to get enough energy to realize impact ionization. On the other hand, if the breakdown is related to the surface states (surface breakdown), V_{BD} will have a negative temperature dependence because hopping conduction through surface states is more significant at higher temperature. Figure 5(b) presents the V_{BD} and leakage current as a function of temperature. It's observed that V_{BD} decreases with increasing operating temperatures, indicating that the breakdown is indeed surface breakdown. This is further supported by our XPS data above showing that large amount of surface states are present on the n-AlN sample. Wu and Kahn [32] and Miao *et al.* [33] confirmed that the surface states on AlN are associated with Al dangling bonds by photoemission spectroscopy and density-functional theory (DFT), respectively. Reddy *et al.* [23] also characterized the surface states on AlN by XPS and found the density of surface states on AlN is larger than that on GaN. In addition, surface states are also commonly observed in other III-nitride devices such as GaN HEMTs and considerably influence device performances [34], [35]. Therefore, surface leakage through these surface states may be the major contributor to the device breakdown mechanism.

Figure 6 presents both experimental and theoretical results of temperature-dependent reverse leakage current at various biases. There could be several mechanisms responsible for the reverse leakage current, including thermionic emission, trap-assisted tunneling, Frenkel-Poole (FP) emission and VRH. Due to the high Schottky barrier height of ~2.2 eV, leakage current through thermionic emission would be negligibly small. The leakage currents have a strong dependence on temperature, which implies tunneling is not the dominate

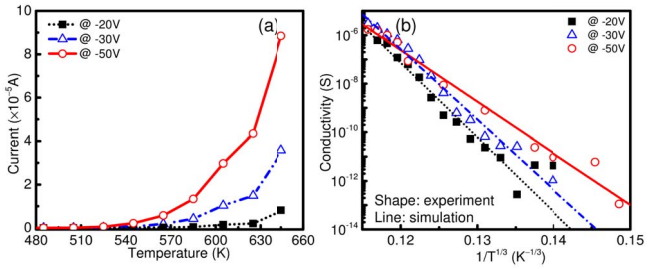

FIGURE 6. **(a) Temperature-dependent reverse leakage current at voltages of −20 V, −30 V and −50 V, and (b) conductivity as a function of 1/T1/3 at different reverse voltages for AlN Schottky diode. 2D-VRH conduction model is used to fit the experimental data.**

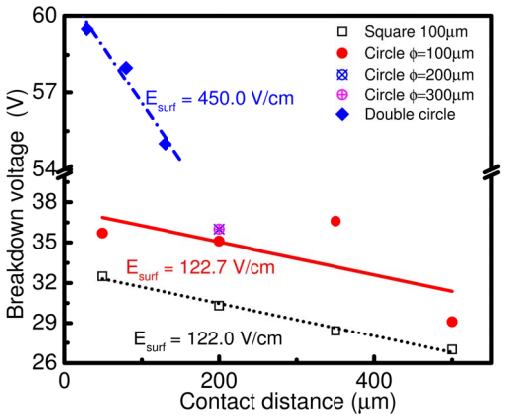

FIGURE 7. **Breakdown voltage as a function of contact distance between ohmic and Schottky contacts for AlN Schottky diodes with different geometries.**

transport mechanism and some other thermally activated conduction mechanisms are needed [36]. One possible model for the leakage current is 2D-VRH conduction assisted by surface states. In this model, the conductivity is expressed as [37]:

$$\sigma = \sigma_0 exp\left[-(T_1/T)^{1/3}\right] \quad (2)$$

where σ_0 is a constant and T_1 is the characteristic temperature. In Fig. 6(b), we plot the measured conductivities of our AlN Schottky diode as a function of $1/T^{1/3}$ in the log scale, where apply linear fitting using the 2D-VRH model was applied. A very good agreement between the experimental data and modeling data was obtained. This indicates that the reverse leakage current is indeed governed by 2D-VRH through the surface states. It may also be argued that trap-assisted tunneling is also temperature dependent, which is proportional to exp(E_A/kT) where E_A is thermal activation energy. Fitting the experimental data with this model yielded E_A over 1 eV, which is far larger than the thermal energy (0.026 eV) at room temperature. This indicates the thermal activation process is highly inefficient and trap-assisted tunneling only contributes a small amount of current to the total leakage currents. In terms of FP emission model, the fitting result revealed that the measured I-V curves didn't follow the relation of $I \propto \exp(V^{1/2})$ [38] at all the measured temperatures. In addition, it's also reported that FP emission process is relatively weak compared with VRH due to long electron emission time in III-nitride devices [39]. Based on discussions from both temperature-dependent V_{BD} and leakage current, surface states may play an important role in determining the reverse voltage breakdown and current leakage of AlN Schottky diodes, especially at high temperatures.

To quantitatively characterize the reverse breakdown voltage and leakage current at high temperatures, I–V characteristics of square (side length of 100 μm) and circular (ϕ = 100μm) Schottky diodes were measured at 500 K. Figure 7 summaries the results on V_{BD} for the two types of AlN Schottky diodes, where the results from donut-shaped Schottky diodes are also shown for comparison. Several important implications can be obtained by analyzing Fig. 7. First, different V_{BD}values were obtained for various devices, in decreasing order of: double circle > circle > square. Square AlN Schottky diodes showed the lowest V_{BD}, which can be explained by the electric field crowding effect at the sharp edges of the square Schottky contacts that facilitates the surface breakdown through nonuniform current spreading and overheating of the devices. This phenomenon is consistent with reports on other III-nitride power electronics [40], [41]. The donut-shaped double circle Schottky diodes have the most evenly distributed electric fields due to the device shape, leading to the highest V_{BD}.

Second, the V_{BD} of the AlN Schottky diodes showed a small dependence on the Schottky contact area of the devices. Schottky diodes fabricated on other wide bandgap semiconductors such as GaN and SiC typically exhibit a contact-area-dependence of V_{BD}, i.e., decreasing of V_{BD} with larger Schottky contact. This is attributed to the defects at device active region, i.e., the interface between Schottky contact and GaN/SiC, and/or the Schottky contact periphery. These defects serve as initiation catalysts for carrier multiplications, leading to premature breakdown [42]–[44]. Therefore, devices with larger Schottky contacts will have higher probability of finding defects in their active region, thus having smaller V_{BD} [45]. However, very similar V_{BD}values were obtained in our study for the three circular AlN Schottky diodes with different diameters (ϕ = 100, 200 and 300 μm, respectively) and the same contact distance of 200 μm, which is different from GaN or SiC Schottky diodes. This indicates that the surface distance or surface area of AlN Schottky diodes has a stronger impact on the V_{BD} than their device contact area, especially when surface breakdown is dominant. This distinct device behavior on AlN Schottky diodes (compared to GaN or SiC devices) can be contributed to the different polarity and surface property of AlN material. For example, AlN is a stronger polar material and thus has larger amount of surface states than GaN [23]. Therefore, the performance of lateral AlN Schottky diodes may be dominated by the surface distance or surface area (i.e., surface

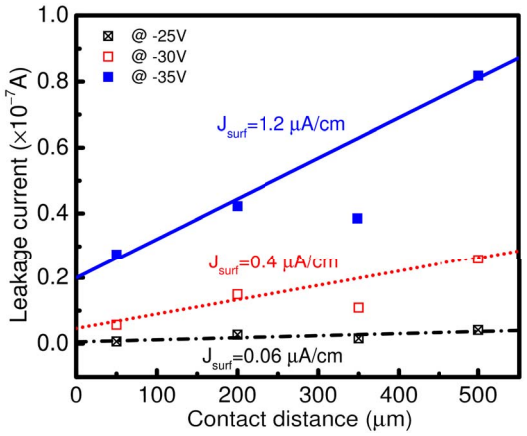

FIGURE 8. Leakage current as a function of contact distance between ohmic and Schottky contacts for square AlN Schottky diode at different reverse voltages.

states) between the ohmic and Schottky contacts, while the Schottky/semiconductor interface may have a smaller effect on the device performances.

Third, the V_{BD} of the AlN Schottky diodes decreases with increasing surface distance between the ohmic and Schottky contacts. In contrast to GaN Schottky diodes where the Schottky contact area has a strong effect on device performances, in AlN Schottky diodes, the surface distance or the surface area between the ohmic and Schottky contacts, will play a more significant role. Devices with larger contact distances are more likely to have bad surfaces with more surface states between the ohmic and Schottky contacts. As a result, the surface leakage current increases with the contact distance and larger devices have smaller V_{BD}. This is analogous to the reason for contact-area-dependence of V_{BD} for GaN devices. This trend may be reserved when these surface states are effectively passivated and further investigations are undergoing. Another possible mechanism is related to the poor material quality. Because the AlN epilayer has a high defect density of $>10^9$ cm^{-2}, there is a high probability of having random defects in large devices. Therefore, the V_{BD} for the larger devices can be lower than that of smaller devices. It's also noteworthy that the performance of donut-shaped AlN Schottky diodes showed a stronger contact-distance dependence than both square and circular devices. This can be characterized by the surface breakdown electric field E_{surf}, which was obtained for various devices using a linear fitting. E_{surf} of 450.0 V/cm, 122.7 V/cm, and 122.0 V/cm were obtained for double circle Schottky diodes, circular Schottky diodes, and square Schottky diodes, respectively. The donut-shaped AlN Schottky diodes have a larger device surface area than the square and the circular Schottky diodes with the same contact distance (the former is radial while the latter is unidirectional), leading to more surface states and stronger dependence of device performances on the contact distances.

Figure 8 shows the leakage current for square AlN Schottky diodes as a function of contact distance at voltages of −25V, −30V, and −35V. Using linear fitting, we obtain surface leakage currents J_{surf} of 1.2μA/cm at −35V, 0.4 μA/cm at −30 V, and 0.06 μA/cm at −25 V, values which are comparable with those obtained on other material systems [46]. The reverse leakage current of the AlN Schottky diodes increased with contact distance. With shorter contact distance, there is less chance of having a bad surface area between the contacts. As a result, the surface leakage current increases with the contact distance. In addition, the relatively poor material quality may also play a role since larger devices are more likely to have random defects and thus larger leakage current. At higher reverse bias, the leakage current also increased because the hopping conduction is driven by the electric field [37]. The current leakage is expected to be suppressed by MOCVD growth optimization to improve crystal quality and reduce defect density. Other surface treatments (such as acids and plasmas) and surface passivation techniques using SiO_2, SiNx and Al_2O_3 may also contribute to reducing current leakage and enhancing breakdown voltage of AlN devices, which are undergoing research topics.

IV. CONCLUSION

Lateral Pd/n-AlN Schottky diodes were fabricated without passivation on a sapphire substrate using MOCVD and metal deposition. The temperature-dependent forward and reverse I–V characteristics were obtained for various AlN Schottky diodes, followed by rigorous analysis. At forward bias, the expected lateral non-uniformities in the Schottky barrier height led to the large ideality factors for the devices. The negative temperature-dependence of reverse V_{BD} indicates that the breakdown mechanism is related to surface states. The reverse leakage current was described using the surface-states-assisted 2D-VRH conduction model, and a good agreements was achieved between the experimental and the theoretical results. Moreover, the V_{BD} and leakage current exhibited strong dependence on the contact distance, showing the device performances of AlN Schottky diodes are strongly dominated by the surface states between the ohmic and Schottky contacts. Finally, the surface breakdown electric field and the leakage current were quantitatively characterized for the AlN Schottky diodes, and E_{surf} of 122–450 V/cm and J_{surf} of 0.4 μA/cm at -30 V were obtained. These results suggest that surface states play significant roles in the device performance of AlN Schottky diodes. Proper passivation and surface treatment techniques may further improve the device performances of AlN Schottky diodes and have an impact on the reverse breakdown and current leakage mechanisms.

REFERENCES

[1] S. Nakamura, G. Fasol, and S. J. Pearton, *The Blue Laser Diode: The Complete Story*, 2nd ed. Berlin, Germany: Springer, 2000.

[2] C.-C. Pan *et al.*, "High optical power and low-efficiency droop blue light-emitting diodes using compositionally step-graded InGaN barrier," *Electron. Lett.*, vol. 51, no. 15, pp. 1187–1189, Jul. 2015.
[3] H. Chen *et al.*, "Optical cavity effects in InGaN micro-light-emitting diodes with metallic coating," *IEEE Photon. J.*, vol. 9, no. 3, p. 8200808, Jun. 2017.
[4] Z. Lu *et al.*, "Active tracking system for visible light communication using a GaN-based micro-LED and NRZ-OOK," *Opt. Exp.*, vol. 25, no. 15, p. 17971–17981, Jul. 2017.
[5] H. Fu *et al.*, "Study of low efficiency droop in semipolar (20-2-1) InGaN light-emitting diodes by time-resolved photoluminescence," *J. Display Technol.*, vol. 12, no. 7, pp. 736–741, Jul. 2016.
[6] H. Fu, Z. Lu, and Y. Zhao, "Analysis of low efficiency droop of semipolar InGaN quantum well light-emitting diodes by modified rate equation with weak phase-space filling effect," *AIP Adv.*, vol. 6, no. 6, 2016, Art. no. 065013.
[7] H. Chen, H. Fu, Z. Lu, X. Huang, and Y. Zhao, "Optical properties of highly polarized InGaN light-emitting diodes modified by plasmonic metallic grating," *Opt. Exp.*, vol. 24, no. 10, pp. A856–A867, May 2016.
[8] X. Huang *et al.*, "Analysis of loss mechanisms in InGaN solar cells using a semi-analytical model," *J. Appl. Phys.*, vol. 119, no. 21, Jun. 2016, Art. no. 213101.
[9] X. Huang *et al.*, "Nonpolar and semipolar InGaN/GaN multiple-quantum-well solar cells with improved carrier collection efficiency," *Appl. Phys. Lett.*, vol. 110, no. 16, Apr. 2017, Art. no. 161105.
[10] H. Chen *et al.*, "Characterizations of nonlinear optical properties on GaN crystals in polar, nonpolar, and semipolar orientations," *Appl. Phys. Lett.*, vol. 110, no. 18, May 2017, Art. no. 181110.
[11] H. Fu, Z. Lu, X. Huang, H. Chen, and Y. Zhao, "Crystal orientation dependent intersubband transition in semipolar AlGaN/GaN single quantum well for optoelectronic applications," *J. Appl. Phys.*, vol. 119, no. 17, May 2016, Art. no. 174502.
[12] H. Fu, H. Chen, X. Huang, Z. Lu, and Y. Zhao, "Theoretical analysis of modulation doping effects on intersubband transition properties of semipolar AlGaN/GaN quantum well," *J. Appl. Phys.*, vol. 121, no. 1, Jan. 2017, Art. no. 014501.
[13] Y.-F. Wu *et al.*, "Very-high power density AlGaN/GaN HEMTs," *IEEE Trans. Electron Devices*, vol. 48, no. 3, pp. 586–590, Mar. 2001.
[14] K. Nomoto *et al.*, "1.7-kV and 0.55- mΩ cm^2 GaN p-n diodes on bulk GaN substrates with avalanche capability," *IEEE Electron Device Lett.*, vol. 37, no. 2, pp. 161–164, Feb. 2016.
[15] H. Fu *et al.*, "Effect of buffer layer design on vertical GaN-on-GaN p-n and Schottky power diodes," *IEEE Electron Device Lett.*, vol. 38, no. 6, pp. 763–766, Jun. 2017.
[16] Y. Cao *et al.*, "High-voltage vertical GaN Schottky diode enabled by low-carbon metal-organic chemical vapor deposition growth," *Appl. Phys. Lett.*, vol. 108, no. 6, Feb. 2016, Art. no. 062103.
[17] Y. Irokawa, E. A. G. Villora, and K. Shimamura, "Shottky barrier diodes on AlN free-standing substrates," *Jpn. J. Appl. Phys.*, vol. 51, no. 4, Mar. 2012, Art. no. 040206.
[18] T. Kinoshita *et al.*, "Fabrication of vertical Schottky barrier diodes on n-type freestanding AlN substrates grown by hydride vapor phase epitaxy," *Appl. Phys. Exp.*, vol. 8, no. 6, May 2015, Art. no. 061003.
[19] H. Fu *et al.*, "Demonstration of AlN Schottky barrier diodes with blocking voltage over 1 kV," *IEEE Electron Device Lett.*, vol. 38, no. 9, pp. 1286–1289, Sep. 2017.
[20] S. M. Evans *et al.*, "Electron paramagnetic resonance of a donor in aluminum nitride crystals," *Appl. Phys. Lett.*, vol. 88, no. 6, Feb. 2006, Art. no. 062112.
[21] Y. A. Xi *et al.*, "Very high quality AlN grown on (0001) sapphire by metal-organic vapor phase epitaxy," *Appl. Phys. Lett.*, vol. 89, no. 10, Sep. 2006, Art. no. 103106.
[22] T. Y. Wang, J. H. Liang, G. W. Fu, and D. S. Wuu, "Defect annihilation mechanism of AlN buffer structures with alternating high and low V/III ratios grown by MOCVD," *CrystEngComm*, vol. 18, no. 47, pp. 9152–9159, Nov. 2016.
[23] P. Reddy *et al.*, "The effect of polarity and surface states on the Fermi level at III-nitride surfaces," *J. Appl. Phys.*, vol. 116, no. 12, Sep. 2014, Art. no. 123701.
[24] A. Rizzi and H. Luth, "Comment on 'influence of crystal polarity on the properties of Pt/GaN Schottky diodes' [Appl. Phys. Lett. 77, 2012 (2000)]," *Appl. Phys. Lett.*, vol. 80, no. 3, p. 530, Jan. 2002.
[25] J. R. Waldrop and R. W. Grant, "Formation and Schottky barrier height of metal contacts to $\beta-$SiC," *Appl. Phys. Lett.*, vol. 56, no. 6, p. 557–559, Jan. 1990.
[26] G. Ye, H. Wang, and R. Ji, "Band alignment of HfO_2/AlN heterojunction investigated by X-ray photoelectron spectroscopy," *Appl. Phys. Lett.*, vol. 108, no. 16, Apr. 2016, Art. no. 162103.
[27] P. Reddy *et al.*, "Schottky contact formation on polar and non-polar AlN," *J. Appl. Phys.*, vol. 116, no. 19, Nov. 2014, Art. no. 194503.
[28] F. Iucolano, F. Roccaforte, F. Giannazzo, and V. Raineri, "Barrier inhomogeneity and electrical properties of Pt/GaN Schottky contacts," *J. Appl. Phys.*, vol. 102, no. 11, Dec. 2007, Art. no. 113701.
[29] F. Iucolano, F. Roccaforte, F. Giannazzo, and V. Raineri, "Temperature behavior of inhomogeneous Pt/GaN Schottky contacts," *Appl. Phys. Lett.*, vol. 90, no. 9, Feb. 2007, Art. no. 092119.
[30] F. Ren *et al.*, "Surface and bulk leakage currents in high breakdown GaN rectifiers," *Solid State Electron.*, vol. 44, no. 4, pp. 619–622, Apr. 2000.
[31] Y. Ohno, T. Nakao, S. Kishimoto, K. Maezawa, and T. Mizutani, "Effects of surface passivation on breakdown of AlGaN/GaN high-electron-mobility transistors," *Appl. Phys. Lett.*, vol. 84, no. 12, pp. 2184–2186, Mar. 2004.
[32] C. I. Wu and A. Kahn, "Electronic states at aluminum nitride (0001)-1×1 surfaces," *Appl. Phys. Lett.*, vol. 74, no. 4, p. 546, Jan. 1999.
[33] M. S. Miao, A. Janotti, and C. G. Van de Walle, "Reconstructions and origin of surface states on AlN polar and nonpolar surfaces," *Phys. Rev. B, Condens. Matter*, vol. 80, no. 15, Oct. 2009, Art. no. 155319.
[34] B. M. Green *et al.*, "The effect of surface passivation on the microwave characteristics of undoped AlGaN/GaN HEMTs," *IEEE Electron Device Lett.*, vol. 21, no. 6, pp. 268–270, Jun. 2000.
[35] J. P. Ibbetson *et al.*, "Polarization effects, surface states, and the source of electrons in AlGaN/GaN heterostructure field effect transistors," *Appl. Phys. Lett.*, vol. 77, no. 2, pp. 250–252, Jul. 2000.
[36] E. J. Miller, E. T. Yu, P. Waltereit, and J. S. Speck, "Analysis of reverse-bias leakage current mechanisms in GaN grown by molecular-beam epitaxy," *Appl. Phys. Lett.*, vol. 84, no. 4, pp. 535–537, Jan. 2004.
[37] D. Yu, C. Wang, B. L. Wehrenberg, and P. Guyot-Sionnest, "Variable range hopping conduction in semiconductor nanocrystal solids," *Phys. Rev. Lett.*, vol. 92, no. 21, May 2004, Art. no. 216802.
[38] J. Kim *et al.*, "Investigation of reverse leakage characteristics of InGaN/GaN light-emitting diodes on silicon," *IEEE Electron Device Lett.*, vol. 33, no. 12, pp. 1741–1743, Dec. 2012.
[39] L. Zhao *et al.*, "Tunneling-hopping transport model for reverse leakage current in InGaN/GaN blue light-emitting diodes," *IEEE Photon. Technol. Lett.*, vol. 29, no. 17, pp. 1447–1450, Sep. 1, 2017.
[40] H. Xing *et al.*, "High breakdown voltage AlGaN-GaN HEMTs achieved by multiple field plates," *IEEE Electron Device Lett.*, vol. 25, no. 4, pp. 161–163, Apr. 2004.
[41] Z. Z. Bandić *et al.*, "High voltage (450 V) GaN Schottky rectifiers," *Appl. Phys. Lett.*, vol. 74, no. 9, p. 1266, Mar. 1999.
[42] P. G. Neudeck, "Progress in silicon carbide semiconductor electronics technology," *J. Electron. Mater.*, vol. 24, no. 4, pp. 283–288, Apr. 1995.
[43] Y. Zhou *et al.*, "Electrical characteristics of bulk GaN-based Schottky rectifiers with ultrafast reverse recovery," *App. Phys. Lett.*, vol. 88, no. 11, Mar. 2006, Art. no. 113509.
[44] B. S. Kang *et al.*, "Temperature dependent characteristics of bulk GaN Schottky rectifiers on free-standing GaN substrates," *J. Vac. Sci. Technol. B*, vol. 22, no. 2, pp. 710–714, Mar. 2004.
[45] Y. Zhou *et al.*, "High breakdown voltage Schottky rectifier fabricated on bulk n-GaN substrate," *Solid State Electron.*, vol. 50, nos. 11–12, pp. 1744–1747, Nov./Dec. 2006.
[46] T. H. Loh *et al.*, "Selective epitaxial germanium on silicon-on-insulator high speed photodetectors using low-temperature ultrathin $Si_{0.8}Ge_{0.2}$buffer," *Appl. Phys. Lett.*, vol. 91, no. 7, Aug. 2007, Art. no. 073503.

HOUQIANG FU is currently pursuing the Ph.D. degree with the School of Electrical, Computer, and Energy Engineering, Arizona State University, USA. His research interests are in the fields of III-nitride power electronics, optoelectronics, optical devices, and visible light communication.

XUANQI HUANG is currently pursuing the Ph.D. degree with the School of Electrical, Computer, and Energy Engineering, Arizona State University, USA. His research interests are in the fields of III-nitride power electronics, optoelectronics, optical devices, and visible light communication.

HONG CHEN is currently pursuing the Ph.D. degree with the School of Electrical, Computer, and Energy Engineering, Arizona State University, USA. His research interests are in the fields of III-nitride power electronics, optoelectronics, optical devices, and visible light communication.

ZHIJIAN LU is currently pursuing the Ph.D. degree with the School of Electrical, Computer, and Energy Engineering, Arizona State University, USA. His research interests are in the fields of III-nitride power electronics, optoelectronics, optical devices, and visible light communication.

YUJI ZHAO received the Ph.D. degree in electrical and computer engineering from the University of California at Santa Barbara (UCSB), in 2012, where he was an Assistant Project Scientist with the Solid State Lighting and Energy Center, UCSB. He joined ASU, in 2014, where he is currently an Assistant Professor. His research focus on advanced electronic and optoelectronic devices based on wide bandgap III-nitride semiconductors.